# Fluorescent core-shell silica nanoparticles as tunable precursors: towards encoding and multifunctional nano-probes†‡

**Chuanliu Wu,[a] Jinqing Hong,[a] Xiangqun Guo,[a] Chaobiao Huang,[b] Jinping Lai,[a] Jinsheng Zheng,[a] Jianbin Chen,[a] Xue Mu[a] and Yibing Zhao*[a]**

*Received (in Cambridge, UK) 5th November 2007, Accepted 28th November 2007*
*First published as an Advance Article on the web 10th December 2007*
**DOI: 10.1039/b717038f**



**Core-shell silica nanoparticles comprised of a RuBpy doped silica core and a Pas-DTPA doped silica shell were synthesized and post-functionalized with an encoding fluorescence combination and multiplex imaging function.**

Multiplex bioanalysis possesses several advantages over single-target detection.[1] Encoding silica nanoparticles prepared *via* changing the type and concentration of the doped dyes are one of the most common fluorescent nano-probes which have recently been used for multiplex bioanalysis.[1–3] However, the variation of the type or concentration of the doped dyes can influence the process of the preparation, and even probably leads to the reduction of the homogeneousness and reproduction of the prepared silica nanoparticles.[3] Thus, the quest to prepare encoding silica nano-probes with higher homogeneousness is of extreme significance.

In addition to the well-developed encoding silica nano-probes, recently, multifunctional nano-materials have also become an especially attractive research field.[4–6] The development of multi-functional nano-probes for MRI and subsequent fluorescence imaging has been significant to the diagnosis of tumors and surgical resection.[5,6] Gadolinium doped fluorescent nanoparticles have recently been explored as feasible nano-probes to satisfy this urgent requirement.[6] A silica matrix allows doping of a wide variety of fluorescent dyes and gadolinium chelates, which make it an ideal material for multifunctional bioimaging applications.[6c–e] Explore the design and preparation methods of this type of multifunctional nano-probes would be of great value to their future applications.

Recently, we have proposed a post-encoding concept to the design and preparation of encoding fluorescent probes, which makes the preparation process of multicolor fluorescent spheres rather laborsaving and efficient.[7] As a proof of this concept, a hybrid silica-nanocrystal–organic dye superstructure (HSNOS) has been successfully used as precursor for the preparation of multicolor fluorescent spheres.[7] However, it is not easy to fabricate HSNOS with nano-scale and multifunctionality, which limits its applications in nanostructural biological systems and multifunctional bioimaging. Herein, we present a well-designed core-shell silica nanoparticle as a tunable precursor towards encoding and multifunctional nano-probes. A novel post-functionalization strategy (Scheme 1) has been subsequently proposed to endow this core-shell silica nanoparticle with an encoding fluorescence combination and a multiplex imaging function.

Core-shell silica nanoparticles which comprise of a tris (2, 2′-bipyridyl) dichlororuthenium(II) (RuBpy) doped silica core and a Pas-DTPA (Molecular structure is shown in Scheme 1) doped silica shell were synthesized in two steps using a water-in-oil microemulsion system.[8] High resolution transmission electron microscopy (TEM) was used for the characterization of the preparation of core-shell architectural silica nanoparticles. Fig. 1a shows an example of TEM images of RuBpy doped silica cores. The diameter of the silica cores is 49 ± 3 nm. TEM images of the ultimate core-shell architectural silica nanoparticles were shown in Fig. 1b. The average diameter of the nanoparticles is 71 ± 4 nm. HRTEM image shown in the inset of Fig. 1b and the particle size distribution diagram shown in Fig. 1c both confirms the formation of core-shell architecture. The Pas-DTPA doped silica shell thickness is evaluated to be 11 nm.

Lanthanide ions exhibit low emission quantum yields because of the very low absorption coefficients. For luminescent applications, emission yields of lanthanide ions are typically enhanced by combining with a chelate ligand.[9] Many lanthanide chelate ligands have been made, and Pas-DTPA used here shown in Scheme 1 is a common chelate ligand for $Tb^{3+}$ ions.[9c] Pas-DTPA contains two parts: an organic chromophore (Pas) and a chelate (DTPA). The chelate serves as a scaffold for attaching lanthanide ions in close proximity to the organic chromophore (Pas). It is worth to note that DTPA can combine quasi-irreversibly with lanthanide, such as $Tb^{3+}$ and $Gd^{3+}$ ions.[10] Thus, our core-shell silica nanoparticles

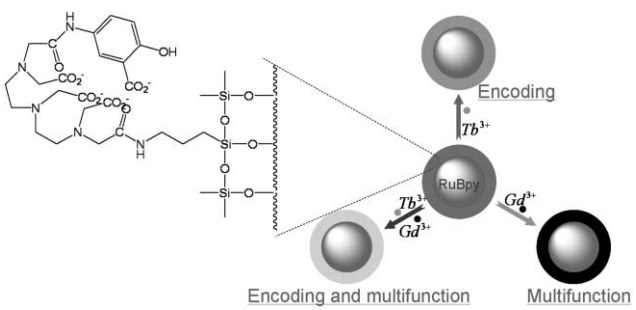


**Scheme 1** Schematic diagram showing the post-functionalization strategy.

[a]*Department of Chemistry and the Key Laboratory of Analytical Sciences of the Ministry of Education, College of Chemistry and Chemical Engineering, Xiamen University, Xiamen, Fujian, P.R. China. E-mail: cooliu6@yahoo.com.cn; Fax: +86-592-2181637; Tel: +86-592-2181637*
[b]*Department of Chemistry, Zhejiang Normal University, Jinhua, Zhejiang, P. R. China*
† Electronic supplementary information (ESI) available: Details of experimental section. See DOI: 10.1039/b717038f
‡ The HTML version of this article has been enhanced with colour images

 

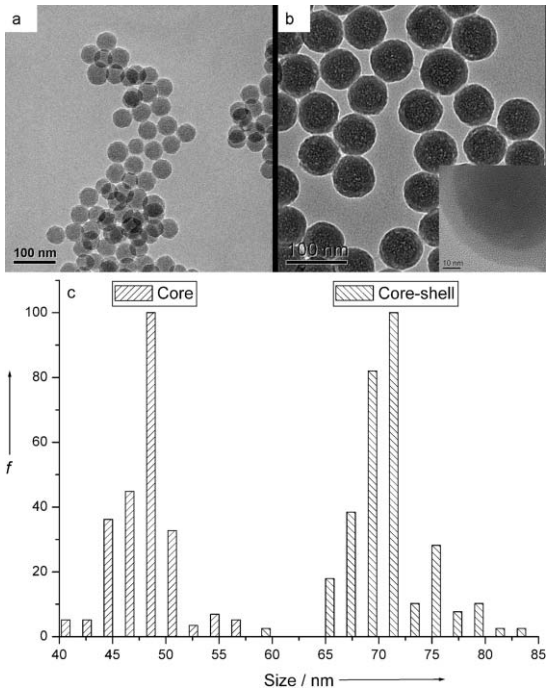


**Fig. 1** (a) TEM images of RuBpy doped silica cores; (b) TEM images of the ultimate core-shell architectural silica nanoparticles, inset: HRTEM image; (c) The particle size distribution diagrams of RuBpy doped silica cores and core-shell silica nanoparticles.

can be post-functionalized by incubating with different concentration of $Tb^{3+}$ and/or $Gd^{3+}$ ions. Fig. 2a shows the fluorometric excitation and emission spectra of Pas-DTPA-Tb and RuBpy. These two inorganic dyes share a broad overlapped excitation spectrum but have two distinct maximum emission wavelengths, with Pas-DTPA-Tb at 545 nm and RuBpy at 585 nm. Fluorescence emission spectra of the core-shell silica nanoparticles incubated with $Tb^{3+}$ ions or not were shown in Fig. 2b. According to the fluorometry studies of the post-functionalized silica nanoparticles, and assuming the density of silica nanoparticles is equal to pure silica,[11] we have estimated that about 3500 $Ru^{2+}$ ions and maximum 2100 $Tb^{3+}$ ions were capable to bind to each nanoparticle. The emergence of fluorescence from $Tb^{3+}$ ions is due to the quasi-irreversible combination of $Tb^{3+}$ with Pas-DTPA. The porous silica matrix and unique core-shell nanoscale architecture make the process of post-functionalization rather efficient.

To endow the core-shell silica nanoparticles with encoding fluorescence combinations, the nanoparticles were incubated with different concentration of $Tb^{3+}$ ions. After approximately 10 h, the incubated nanoparticles were separated by centrifuging. The normalized fluorescence spectra taken from these post-functionalized silica nanoparticles were shown in Fig. 3. As can be seen from Fig. 3, a gradual increase in the fluorescence intensity of $Tb^{3+}$ ions was observed upon addition of increasing amounts of $Tb^{3+}$ ions. Fluorescence intensity ratio of the multiplex emission can be accurately controlled by varying the amounts of the additive $Tb^{3+}$ ions. The inset of Fig. 3 shows the correlation between the intensity ratio at 545 nm to 590 nm and the relevant amounts of the additive $Tb^{3+}$ ions. To determine whether the intensity ratios have batch-to-batch reproducibility, the average peak intensity ratios from five parallel post-functionalized nanoparticle solutions were compared

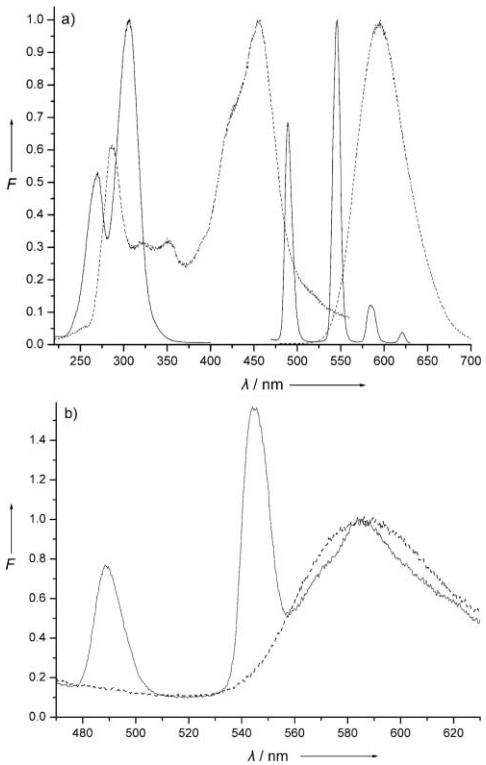


**Fig. 2** (a) Normalized fluorometric excitation and emission spectra of Pas-DTPA-$Tb^{3+}$ (solid lines) and RuBpy (dot lines); (b) The normalized fluorometric emission spectra of the core-shell silica nanoparticles before (dot line) and after (solid line) incubating with $Tb^{3+}$ ions, excitation wavelength: 320 nm.

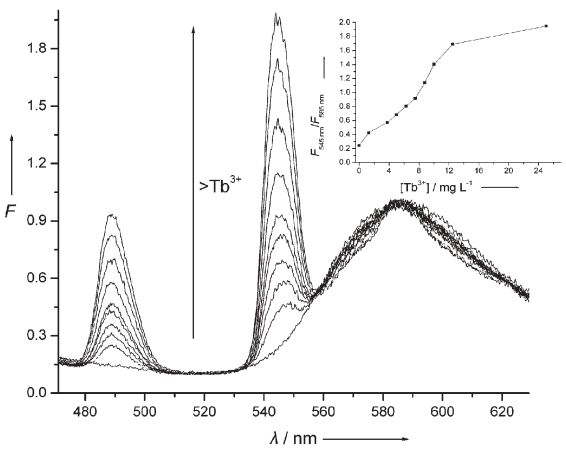


**Fig. 3** Fluorescence emission spectra of encoding silica nanoparticles post-functionalized with $Tb^{3+}$ ions; Inset: Correlation between the intensity ratio and concentration of $Tb^{3+}$ ions.

and the standard deviations for these intensity ratios are less than 3%. This high level of reproducibility allows not only more intensity ratios to be distinguished but also higher precision in the multiplex analysis.

To endow core-shell silica nanoparticles with both encoding fluorescence combination and multiplex imaging function, silica nanoparticles were post-functionalized *via* incubating with different concentration ratios of $Gd^{3+}$ and $Tb^{3+}$ ions. As can be seen

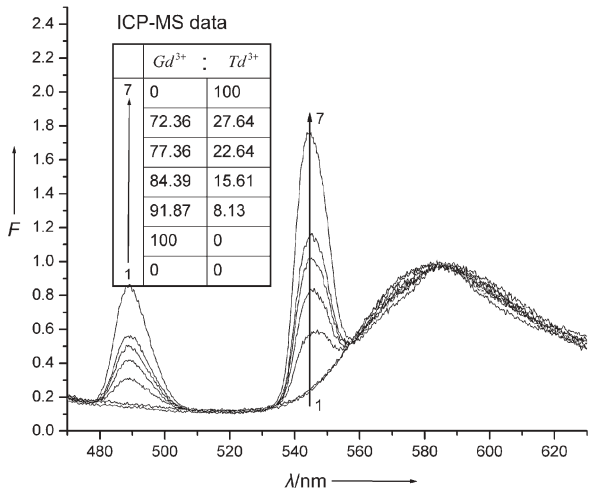


**Fig. 4** Fluorescence emission spectra of encoding and multifunctional silica nanoparticles post-functioned with different concentration ratios of $Tb^{3+}$ and $Gd^{3+}$ ions; inset table: concentration ratios of $Gd^{3+}$ and $Tb^{3+}$ ions determined by ICP-MS.

from the fluorescence spectra (Fig. 4), silica nano-probes with different fluorescence emission (encoding) doped with magnetic resonance (MR) contrast agent (multifunction), $Gd^{3+}$ ions, can be obtained *via* this facile post-functionalization strategy. The inset table of Fig. 4 shows the concentration ratios of $Gd^{3+}$ and $Tb^{3+}$ ions in the encoding and multifunctional silica nanoparticles determined by inductively coupled plasma-mass spectroscopy (ICP-MS). The conclusive ICP-MS data also confirmed the successful binding of $Tb^{3+}$ and $Gd^{3+}$ ions in the silica matrix. Successful doping of plentiful $Gd^{3+}$ ions indicates that the MR contrast enhancement can be reasonably pronounced when the post-functionalized silica nanoparticles are used in MRI. In the present study, although the MRI measurements of multicolor and multifunctional silica nanoparticles were not performed, MR studies of $Gd^{3+}$ shell-doped silica nanoparticles reported by Santra and co-workers have demonstrated that this type of nanoparticle can result in image contrast on both $T_1$- and $T_2$-weighted images to a larger extent than a commonly used MR contrast agent.[6c] Thus, we affirm that our post-functionalized nano-probes could find various biological applications in magnetic resonance imaging and encoding fluorescence multiplex bioanalysis.

For multiplex bioanalysis and multifunctional bioimaging, the dispersion and homogeneousness of the nano-probes are both particularly important criteria. The dispersion of silica nanoparticles has been demonstrated to be very effective because of the high hydrophilicity and biocompatibility of silica.[1a,2,3] The homogeneousness of silica nanoparticles fabricated in different batches or doped with different types or concentration of dyes, however, is difficult to be controlled by existing strategies. Different from existing strategies in the literature, our post-functionalization strategy does not involve the batch-to-batch preparation process as well as the variation in the type or concentration of doped dyes. Thus, the homogeneousness of the encoding and multifunctional nano-probes fabricated *via* the proposed post-functionalization strategy is very high (Fig. 1c), with a relative standard deviation of the particle size less than 6%.

In summary, we have successfully developed a novel post-functionalization strategy to fabricate encoding and multifunctional silica nano-probes. Our post-functionalization strategy does not involve the batch-to-batch preparation process or variation of the type or concentration of doped dyes, which makes the preparation process rather labor saving and efficient and leads to well-controlled size homogeneousness. In addition, the core-shell architectural silica nanoparticles will allow doping of other fluorescent dyes and chelate ligands in the silica core and shell. The post-functionalized nano-probes can also be used in time-gated multiplex bioanalysis because of the long fluorescence lifetime of the two inorganic dyes. It is expected that our post-functionalized nano-probes will find various biological applications in multiplex bioanalysis, fluorescence imaging and MRI.

This research was supported by National Natural Science Foundation of China (No. 20745004).

## Notes and references

1 (*a*) L. Wang, K. Wang, S. Santra, X. Zhao, L. R. Hilliard, J. E. Smith, Y. Wu and W. Tan, *Anal. Chem.*, 2006, **78**, 646; (*b*) R. Wilson, A. R. Cossins and D. G. Spiller, *Angew. Chem., Int. Ed.*, 2006, **45**, 6104.
2 (*a*) L. Wang, C. Yang and W. Tan, *Nano Lett.*, 2005, **5**, 37; (*b*) L. Wang and W. Tan, *Nano Lett.*, 2006, **6**, 84; (*c*) H. Ow, D. R. Larson, M. Srivastava, B. A. Baird, W. W. Webb and U. Wiesner, *Nano Lett.*, 2005, **5**, 113; (*d*) G. A. Lawrie, B. J. Battersby and M. Trau, *Adv. Funct. Mater.*, 2003, **13**, 887.
3 M. Nakamura, M. Shono and K. Ishimura, *Anal. Chem.*, 2007, **79**, 6507.
4 (*a*) P. Debouttière, S. Roux, F. Vocanson, C. Billotey, O. Beuf, A. Favre-Réguillon, Y. Lin, S. Pellet-Rostaing, R. Lamartine, P. Perriat and O. Tillement, *Adv. Funct. Mater.*, 2006, **16**, 2330; (*b*) S. Santra, H. Yang, P. H. Holloway, J. T. Stanley and R. A. Mericle, *J. Am. Chem. Soc.*, 2005, **127**, 1656; (*c*) B. G. Trewyn, S. Giri, I. I. Slowing and V. S.-Y. Lin, *Chem. Commun.*, 2007, 3236.
5 (*a*) M. F. Kircher, U. Mahmood, R. S. King, R. Weissleder and L. Josephson, *Cancer Res.*, 2003, **63**, 8122; (*b*) S. Wang, B. R. Jarrett, S. M. Kauzlarich and A. Y. Louie, *J. Am. Chem. Soc.*, 2007, **129**, 3848; (*c*) J. Kim, S. Park, J. E. Lee, A. M. Jin, J. H. Lee, I. S. Lee, I. Yang, J. S. Kim, S. K. Kim, M. H. Cho and T. Hyeon, *Angew. Chem., Int. Ed.*, 2006, **45**, 7754; (*d*) C. W. Lu, Y. Hung, J. K. Hsiao, M. Yao, T. H. Chung, Y. S. Lin, S. H. Wu, S. C. Hsu, H. M. Liu, C. Y. Mou, C. S. Yang, D. M. Huang and Y. C. Chen, *Nano Lett.*, 2007, **7**, 149.
6 (*a*) L. Prinzen, R. J. J. H. M. Miserus, A. Dirhsen, T. M. Hackeng, N. Deckers, N. J. Bitsch, R. T. A. Megens, K. Douma, J. W. Heemskerk, M. E. Kooi, P. M. Frederik, D. W. Slaaf, M. A. M. J. Zandvoort and C. P. M. Reutelingsperger, *Nano Lett.*, 2007, **7**, 93; (*b*) R. Bakalova, Z. Zhelev, I. Aoki, H. Ohba, Y. Imai and I. Kanno, *Anal. Chem.*, 2006, **78**, 5925; (*c*) S. Santra, R. P. Bagwe, D. Dutta, J. T. Stanley, G. A. Walter, W. Tan, B. M. Moudgil and R. A. Mericle, *Adv. Mater.*, 2005, **17**, 2165; (*d*) J. L. Bridot, A. C. Faure, S. Laurent, C. Rivière, C. Billotey, B. Hiba, M. Janier, V. Josserand, J. L. Coll, L. V. Elst, R. Muller, S. Roux, P. Perriat and O. Tillement, *J. Am. Chem. Soc.*, 2007, **129**, 5076; (*e*) J. S. Kim, W. J. Rieter, K. M. L. Taylor, H. An, W. Lin and W. Lin, *J. Am. Chem. Soc.*, 2007, **129**, 8962.
7 C. Wu, J. Zheng, C. Huang, J. Lai, S. Li, C. Chen and Y. Zhao, *Angew. Chem., Int. Ed.*, 2007, **46**, 5393.
8 R. P. Bagwe, C. Yang, L. R. Hilliard and W. Tan, *Langmuir*, 2004, **20**, 8336.
9 (*a*) J. R. Lakowicz, Principles of Fluorescence Spectroscopy, 2nd edn, Kluwer/Plenum, New York, 1999, p. 86; (*b*) K. E. Sapsford, L. Berti and I. L. Medintz, *Angew. Chem., Int. Ed.*, 2006, **45**, 4562; (*c*) C. Sun, J. Yang, L. Li, X. Wu, Y. Liu and S. Liu, *J. Chromatogr., B*, 2004, **803**, 173.
10 (*a*) P. Debouttière, S. Roux, F. Vocanson, C. Billotey, O. Beuf, A. Favre-Réguillon, Y. Lin, S. Pellet-Rostaing, R. Lamartine, P. Perriat and O. Tillement, *Adv. Funct. Mater.*, 2006, **16**, 2330; (*b*) A. E. Martele and R. M. Smith, *Critical Stability Constants*, vol. 6, Plenum, New York 1986.
11 Z. Ye, M. Tan, G. Wang and J. Yuan, *Anal. Chem.*, 2004, **76**, 513.

 